PERGAMON

International Journal of Multiphase Flow 29 (2003) 51–67

International Journal of Multiphase Flow

www.elsevier.com/locate/ijmulflow

Critical liquid flows for the transition from the pseudo-slug and stratified patterns to slug flow

A. Soleimani, T.J. Hanratty *

Department of Chemical Engineering, University of Illinois at Urban-Champaign, 205 Roger Adams Laboratory, Box C-3 600 South Mathews Avenue, Urbana, IL 61801, USA

Received 12 December 2001; received in revised form 19 September 2002

Abstract

It has recently been shown that a consideration of the stability of a stratified flow and of the stability of a slug has provided accurate predictions of the critical liquid height of a stratified flow for the transition to a slug or plug flow in horizontal and downwardly inclined pipes. Two diameters and viscosities of 1–70 cp were considered. Predictions of the critical superficial liquid velocity are not so accurate. This paper partially examines this issue by presenting measurements of the mean pressure gradient and of the time-varying holdup for air and water flowing in a horizontal 2.54 cm pipe.

Important contributions are the use of viscous long wavelength theory to predict the initiations of roll waves and the discovery of a range of liquid flows (in the pseudo-slug regime) at which the liquid holdup of the stratified layer is close to the critical and is not changing strongly with liquid flow. A partial explanation for this behavior is given which recognizes that the liquid layer over which roll waves are propagating is below that required for the stability of a slug. Slugs will appear if conditions are favorable for the coalescence of roll waves.

Keywords: Gas–liquid flow; Flow regime transition; Slug flow; Roll waves; Pseudo-slugs

1. Introduction

Two theoretical concepts have played a prominent role in explaining the transition from a stratified to a slug pattern for air–water flow in a horizontal pipe. One of these predicts the critical height at low gas velocities by using viscous long wavelength (VLW) theory to examine the

* Corresponding author. Tel.: +1-217-333-1318; fax: +1-217-333-5052.
E-mail address: hanratty@scs.uiuc.edu (T.J. Hanratty).

PII: S0301-9322(02)00124-6

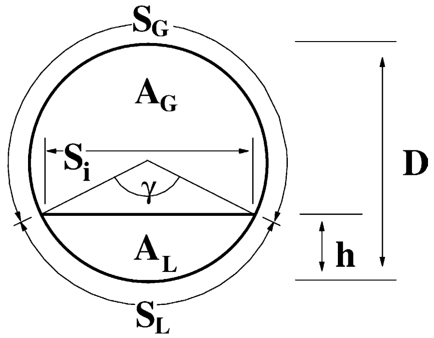

Fig. 1. Simplified geometry for an idealized stratified flow.

stability of a stratified flow (Lin and Hanratty, 1986; Wu et al., 1987). The other predicts the critical height by examining the stability of a slug (Ruder et al., 1989; Bendiksen, 1984; Woods and Hanratty, 1996). A good agreement is noted between predicted and measured critical heights but this is not the case for the critical liquid flow (Hurlburt and Hanratty, 2002). This paper describes experiments aimed at explaining this discrepancy. It is limited in scope in that they are restricted to air and water flowing in a horizontal pipe with a diameter of 2.54 cm. For this case, HH have predicted higher critical liquid flows at low gas velocities and lower critical liquid flows at high gas velocities than are observed in experiments.

Measurements of the time-averaged pressure gradient and liquid holdup were made at a fixed gas rate for different liquid flows. Time-averaged wall shear stresses and interfacial stresses are calculated from the measured time-averaged pressure drop, holdup and gas velocity with the idealized model of a stratified flow (Fig. 1) that is usually employed to develop the relation of liquid holdup to the gas and liquid superficial velocities.

In their study of flow patterns in air–water flows, Lin and Hanratty (1987a,b) defined a pseudo-slug region (in a plot of the superficial gas velocity, U_{SG}, versus the superficial liquid velocity, U_{SL}), near the intersection of the stratified, annular and slug flow regimes. Pseudo-slugs are identified by them as disturbances which have the appearance of slugs, but which do not give the identifying pressure pattern and do not travel at the gas velocity.

Studies of the initiation of slugs in a 2.54 cm pipe are made complicated because the pseudo-slug regime covers a wide range of flow conditions. Lin and Hanratty (1987a,b) show that for $U_{SG} \leqslant 2$ m/s slug flow occurs by a transition from a stratified flow with a relatively smooth interface and that for $2 < U_{SG} < 50$ m/s the transition is from a flow with pseudo-slugs. This paper provides an explanation for the discrepancies in the calculations of HH. However, of equal importance is the provision of new information about the pseudo-slug regime and the demonstration that VLW theory correctly predicts the initiation of roll waves in a pipe flow.

2. Description of the experimental facilities

The experiments were performed in a flow facility described in a number of previous papers (Andritsos and Hanratty, 1987; Fan et al., 1993; Williams, 1990; Woods, 1998). The 2.54 cm pipe

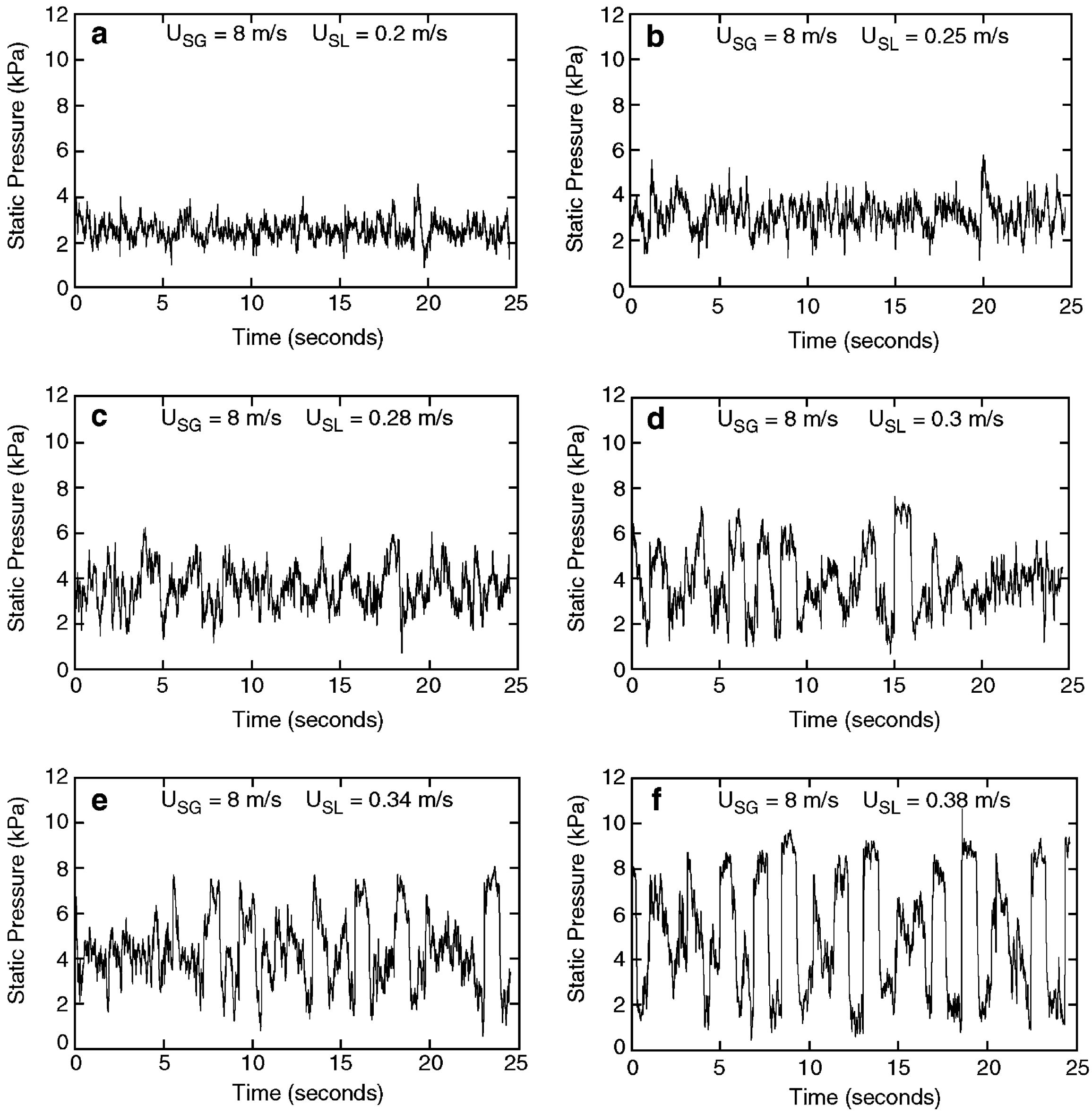

Fig. 2. Pressure pulse measurements at a superficial gas velocity of 8 m/s.

was made of Plexiglas and had a length of 18.3 m. The liquid and gas were mixed in a tee-section at the inlet.

The thickness of the liquid layer, h, flowing along the bottom of the pipe (see Fig. 1) was determined by measuring the conductance between two parallel wires located 15 and 16.5 m from the entrance. The conductance method is described in several previous papers from this laboratory (Lin and Hanratty, 1987a,b; Fan et al., 1993; Woods and Hanratty, 1996). The probes are calibrated by measuring the conductance when the pipe is filled to different levels, h. A plot of h/D versus conductance gives a linear relation (Williams, 1990) so that the time-averaged conductance gives the time-averaged h when the liquid level is varying with time. The conductance between the probes decreases with decreasing conductivity. If bubbles are uniformly distributed in the liquid with a void fraction of ε then the measured h needs to be increased by a fraction $(1 - \varepsilon)$. Fan et al. (1993) have shown that measurements of conductance can be used to obtain the void fraction in slugs.

Pressure gradients were measured with two capacitive differential pressure transducers with pressure ranges of 25 and 625 $\mathrm{N/m^2}$. The taps were placed 15 and 16.5 m from the entrance of the test section. Static pressure fluctuations were measured with another pressure transducer. The flow discharging from the pipe was at atmospheric pressure. Pressure, as well as height measurements, were made every 3 ms.

The initiation of slugs could be identified visually at $U_{\mathrm{SG}} < 5$ m/s. At higher gas velocities, the slugs are not easily differentiated from large amplitude waves. Therefore, visual observations were supplemented with measurements of pressure pulses, as suggested by Lin and Hanratty (1986). An example, for which the critical U_{SL} is 0.25 m/s, is given in Fig. 2. Because of the large pressure difference between the front and the back of a slug there is a sharp pressure increase when the slug passes the measuring point, located 13.3 m from the outlet. If the slug has a velocity of 10 m/s, it reaches the outlet in 1.3 s. A sharp decrease occurs when it discharges from the pipe. Thus, at $U_{\mathrm{SG}} = 10$ m/s, a slug can be identified as a pressure pulse which has a rectangular shape and a length of 1.3 s. About 10 slugs can be seen in Fig. 2f. The heights of the pulses decrease with decreasing slug length, i.e., with decreasing U_{SL}. Taking this into account, slugs can also be identified in Fig. 2c–e. There is some subjectivity in defining the transition, so it is noted that the critical superficial liquid velocities defined in this study agree roughly with previous results obtained by Andritsos and Hanratty (1987) (see Fig. 11).

3. Theory

3.1. A model for a stratified flow pattern

Momentum balances for the gas and liquid flows can be written as follows if the idealized model of a stratified flow is used:

$$-A_{\mathrm{G}}\left(\frac{\mathrm{d}P}{\mathrm{d}x}\right) - \tau_{\mathrm{WG}}S_{\mathrm{G}} - \tau_{\mathrm{i}}S_{\mathrm{i}} + \rho_{\mathrm{G}}A_{\mathrm{G}}g\sin\theta = 0 \tag{1}$$

$$-A_{\mathrm{L}}\left(\frac{\mathrm{d}P}{\mathrm{d}x}\right) - \rho_{\mathrm{l}}g\cos\theta\left(\frac{\mathrm{d}h_{\mathrm{L}}}{\mathrm{d}x}\right) - \tau_{\mathrm{WL}}S_{\mathrm{L}} + \tau_{\mathrm{i}}S_{\mathrm{i}} + \rho_{\mathrm{L}}A_{\mathrm{L}}g\sin\theta = 0 \tag{2}$$

where τ_{WG} and τ_{WL} are the time-averaged resisting stresses of the wall on the gas and liquid phases and τ_{i} is the time-averaged stress at the interface. The simplified geometric representation of the time-averaged stratified flow, that is used in this paper, is given in Fig. 1. The flow is assumed to be horizontal ($\cos\theta = 1$, $\sin\theta = 0$) and fully developed, $\mathrm{d}h/\mathrm{d}x = 0$. The second of these assumptions might not be valid at small gas velocities, where the flow in the liquid is subcritical. The gas phase stress, τ_{WG}, is calculated using the Blasius equation

$$\tau_{\mathrm{WG}} = \frac{f_{\mathrm{BG}} \rho_{\mathrm{G}} U^2}{2} \tag{3}$$

where U is the gas velocity, ρ_{G} is the gas density. The Blasius friction factor for the gas is given by

$$f_{\mathrm{BG}} = 0.0791 \left[\frac{\rho_{\mathrm{G}} U D_{\mathrm{HG}}}{\mu_{\mathrm{G}}} \right]^{-0.25} \tag{4}$$

and D_{HG} is the hydraulic diameter,

$$D_{\mathrm{HG}} = 4 \frac{A_{\mathrm{G}}}{S_{\mathrm{G}} + S_{\mathrm{i}}} \tag{5}$$

Parameters A_{G}, A_{L}, S_{G}, S_{i}, S_{L} can be calculated from measurements of h/D by using geometric formulas presented in Govier and Aziz (1972). Therefore Eqs. (1)–(5) can be used to calculate τ_{i} and τ_{WL} from measurements of $\mathrm{d}P/\mathrm{d}x$ and h/D at a given gas flow.

The interfacial shear stress is expressed in terms of a friction factor, f_{i}, defined as

$$\tau_{\mathrm{i}} = \frac{f_{\mathrm{i}} \rho_{\mathrm{G}} U^2}{2} \tag{6}$$

The wall shear stress in the liquid phase is defined by the equation,

$$\tau_{\mathrm{WL}} = \frac{f_{\mathrm{WL}} \rho_{\mathrm{L}} u^2}{2} \tag{7}$$

where u is the average liquid velocity, ρ_{L} is the liquid density and f_{WL} is the friction factor. For the case of a turbulent flow, the friction factor can be defined by the Blasius equation for the liquid:

$$f_{\mathrm{WL}} = f_{\mathrm{BL}} = 0.0791 \left[\frac{\rho_{\mathrm{L}} U D_{\mathrm{HL}}}{\mu_{\mathrm{L}}} \right]^{-0.25} \tag{8}$$

with

$$D_{\mathrm{HL}} = 4 \frac{A_{\mathrm{L}}}{S_{\mathrm{L}}} \tag{9}$$

For laminar liquid flow the friction factor is approximated as

$$f_{\mathrm{wL}} = \frac{C_{\mathrm{p}}}{Re_{\mathrm{L}}} \tag{10}$$

where, for fully developed laminar flow of a single phase, the Poiseuille parameter, C_{p} equals 16. Russell et al. (1974) have presented results from a numerical solution of the Navier–Stokes equation for a laminar stratified flow with a flat interface and an interfacial stress that is constant along the interface. The pressure gradient was calculated from Eq. (1) with $\sin\theta = 0$. Table 1 presents results from this calculation for the case where τ_{WG} is given by Eqs. (3) and (4) and $\tau_{\mathrm{WG}} = \tau_{\mathrm{i}}$, by tabulating

$$Q^{*} = -\frac{\pi \mu_{\mathrm{L}} V_{\mathrm{SL}}}{2D^2 (\mathrm{d}P/\mathrm{d}x)} \tag{11}$$

Table 1
Laminar liquid–turbulent gas flow for $\tau_i = \tau_{WG}$ (Russell et al., 1974)

Q^*	h/D	C_p
1.58×10^{-4}	0.05	13.1
8.87×10^{-4}	0.10	13.5
4.89×10^{-3}	0.20	13.8
1.28×10^{-2}	0.30	14.0
2.40×10^{-2}	0.40	14.3
3.73×10^{-2}	0.50	14.6
5.08×10^{-2}	0.60	14.9
6.15×10^{-2}	0.70	15.4
6.66×10^{-2}	0.80	16.1
6.31×10^{-2}	0.90	17.2

as a function of h/D. A relation for $Q* = f(h/D)$ can also be developed by using Eqs. (1)–(4), (10). Values for C_p can then be calculated from the results presented by Russell et al. These are given in Table 1.

By eliminating dP/dx between Eqs. (1) and (2) and substituting Eqs. (3)–(10) the following relations are obtained for the superficial liquid velocity if both the liquid and gas phases are turbulent:

$$\left(\frac{U_{SL}}{U_{SG}}\right)^{1.75} = \frac{f_{BL}}{f_{WL}} \frac{\rho_G \mu_G^{0.25}}{\rho_L \mu_L^{0.25}} g_{tt}\left(\frac{h}{D}\right) \tag{12}$$

$$g_{tt}\left(\frac{h}{D}\right) = \left(\frac{A_L}{A_G}\right)^{1.75}\left(\frac{D_{HL}}{D_{HG}}\right)^{0.25}\left\{\frac{S_G A_L}{S_L A_G} + \frac{f_i}{f_{BG}}\frac{S_i}{S_L}\left(1+\frac{A_L}{A_G}\right)\right\} \tag{13}$$

Eq. (12) allows U_{SL} to be calculated if U_{SG} and h/D are known. Similarly, for a turbulent gas and a laminar liquid, the following equations are derived:

$$\left(\frac{U_{SL}}{U_{SG}}\right) = \frac{D^{0.75} U_{SG}^{0.75} \rho_G^{0.75}}{\mu_G^{0.75}}\left(\frac{\mu_G}{\mu_L}\right) g_{tl}\left(\frac{h}{D}\right) \tag{14}$$

$$g_{tl}\left(\frac{h}{D}\right) = \frac{0.0791}{C_p}\frac{A_L}{A}\left(\frac{A}{A_G}\right)^{1.75}\frac{D_{HL}}{D}\left(\frac{D}{D_{HG}}\right)^{0.25}\left\{\frac{S_G A_L}{S_L A_G} + \frac{f_i}{f_{BG}}\frac{S_i}{S_L}\left(1+\frac{A_L}{A_G}\right)\right\} \tag{15}$$

3.2. Viscous long wavelength instability

Hanratty and Hershman (1961) developed VLW stability theory to described the initiation of roll waves in a rectangular channel. The basic assumptions are that the waves are long enough that a hydrostatic approximation can be used to describe the pressure variation in the liquid and that the stresses in the time varying flow can be described by making a pseudo-steady state approximation.

Lin and Hanratty (1986) applied this theory to the complicated flow that exists in a pipe flow. A disturbance is introduced at the interface so that A_L is given by

$$A_L = \overline{A}_L + \widehat{A}_L \exp ik(x - Ct) \tag{16}$$

where the wave number k and the amplitude $\widehat{A}_L$ are real and the wave velocity C is complex. The disturbance is assumed to be small enough that linearized forms of the momentum equation can be used. The real and imaginary parts yield two equations that define $\overline{A}_L$ and C_R for given superficial gas and liquid velocities at neutral stability ($C_I = 0$). Detailed descriptions of these calculations are given in Lin and Hanratty (1986) and in Hurlburt and Hanratty (2002).

3.3. Slug stability model

The stability of a slug is defined by considering the rates at which liquid is picked up at its front and shed at its back. The front of the slug is moving over a stratified flow with a time-averaged area of A_{L1} and a velocity u_1. The stratified flow is assumed to contain no bubbles. The front of the slug, which is moving with a velocity C_F, scoops up the slower moving liquid in the stratified flow at a rate given by

$$Q_{in} = (C_F - u_1)A_{L1} \tag{17}$$

The rear of the slug is pictured to behave as a bubble which has a velocity C_B. The velocity of the liquid in the slug is u_3. The slugs contain air bubbles which are moving at a velocity equal to su_3, where s is the ratio of the bubble velocity to the liquid velocity. The volume fraction of gas in the slug is ε. The slug sheds liquid at a rate

$$Q_{out} = (C_B - u_3)(1 - \varepsilon)A \tag{18}$$

If Q_{in} is greater than Q_{out} the slug will grow. At neutral stability the area of the stratified flow is given by

$$\left(\frac{A_{L1}}{A}\right)_{Crit} = \frac{(C_B - u_3)(1 - \varepsilon)}{C_B - u_1}, \tag{19}$$

From Woods and Hanratty (1996) and Bendiksen (1984) the bubble velocity is given as $C_B = 1.2\ U_{mix} = 1.2(U_{SL} + U_{SG})$ for the experiments reported in this paper (for which the slug is turbulent).

It would not be possible to generate slugs on a stratified flow below this critical value of A_{L1}, so Eq. (19) defines a critical liquid holdup in a stratified flow below which slugs will be unstable. The implementation of Eq. (19) is discussed by Woods and Hanratty (1996) and by Hurlburt and Hanratty (2002). The calculation of the critical liquid holdup for a given U_{SL} and U_{SG} requires expressions for u_3, ε, and s. The liquid velocity in the slug, u_3, is obtained from conservation of mass. The correlation proposed by Andreussi and Bendiksen (1989) was used to calculate ε. Direct measurements of the slip, s, are not available. Woods and Hanratty (1996) used measurements of Q_{out} to calculate s from Eq. (18). These give values of $s \cong 1$ at $U_{mix} < 2$ m/s, $s \cong 1.5$ at $U_{mix} > 8$ m/s and a roughly linear increase between $U_{mix} = 2$ and 8 m/s.

Most often u_1 in Eq. (19) can be ignored because it is much smaller than C_B. In cases where this is not the situation the liquid velocity u_1 can be calculated from momentum balance equations similar to Eqs. (12) and (14) if U_{SG} and the height of the stratified flow between the slugs, h_1, are known.

4. Results

4.1. Time variation of holdup

Figs. 3 and 4 show tracings of the measured time variation of the holdup at $U_{SG} = 3$ and 5 m/s. These are expressed as the ratio of the height of the liquid at mid-plane to the pipe diameter, h/D. At $U_{SG} = 3$ m/s and a superficial liquid velocity, U_{SL}, of 0.01 m/s the interface is relatively smooth. The time-averaged height of the liquid increases with increasing liquid flow. Eventually, roll waves with sharp changes in height in their front and with gradual changes in their backs, such as described by Hanratty and Hershman (1961), appear when $U_{SL} \cong 0.04$ m/s. The h/D is greater than that needed to sustain a stable slug. Because of this, the roll waves have the possibility of growing into a slug. Thus, the slugs appear on the interface at a superficial velocity slightly over the critical flow needed to initiate roll waves. Since the slugs are aerated the h/D in the holdup tracings does not have a value of 1.0. Thus, Fig. 3b indicates roll waves with $h/D \cong 0.6$ and a slug with $h/D \cong 0.8$ at time $\cong$3 s. Fig. 3c shows a mixture of slugs and roll waves.

The tracings for $U_{SG} = 5$ m/s in Fig. 4a shows a stratified flow with small amplitude regular waves. As would be expected, the height of the liquid layer at $U_{SL} = 5$ m/s is smaller than observed at 3 m/s. At a superficial liquid velocity of about 0.025 m/s, roll waves appear at the interface. The height of the base layer is less than that required for a stable slug to exist. Some of these waves can come close to touching the top wall but they do not form stable slugs. They are the pseudo-slugs identified by Lin and Hanratty (1987b). Measurements in Fig. 4b and c at $U_{SL} = 0.05$ m/s and

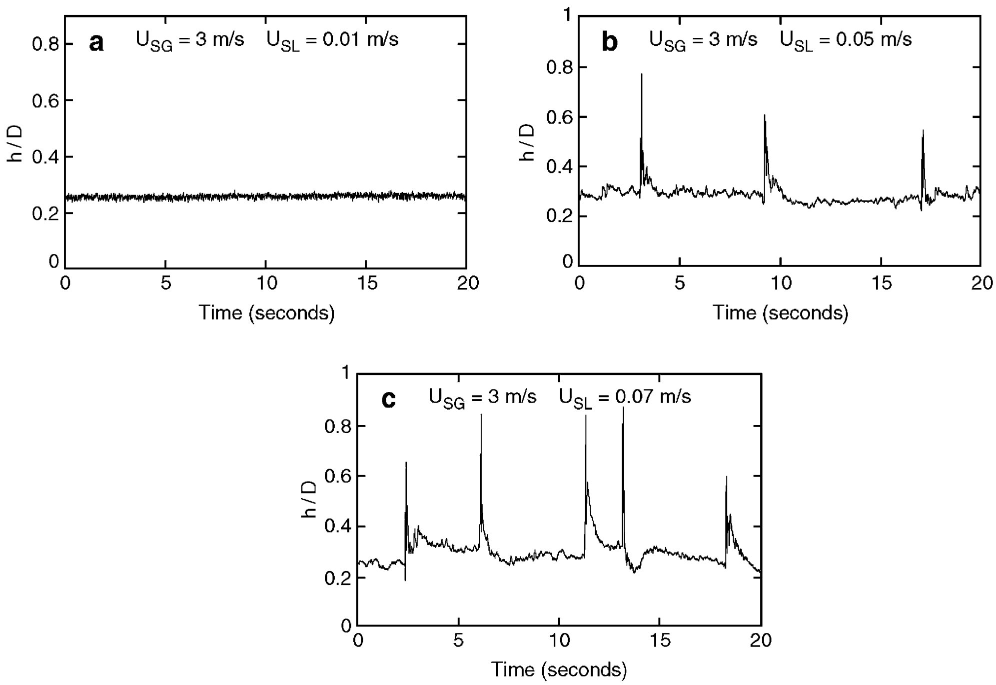

Fig. 3. Liquid holdup measurements at a gas superficial velocity of 3 m/s.

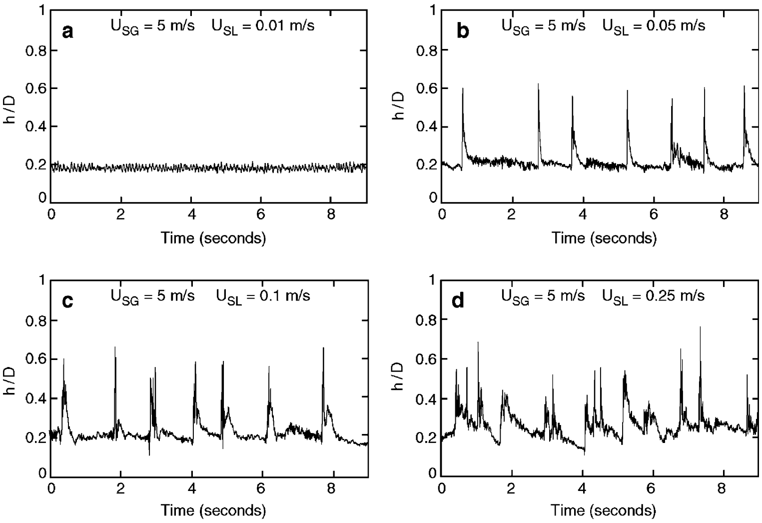

Fig. 4. Liquid holdup measurements at a superficial gas velocity of 5 m/s.

0.1 m/s are examples of this pseudo-slug regime. The base film between these waves is the same as that of the stratified layer prior to transition. An increase in U_{SL} causes an increase in the frequency of these waves but it does not cause an increase in the height of the base film. Thus, the roll waves in Fig. 4b and c do not have the possibility of growing directly into slugs.

Eventually at $U_{SL} \cong 0.18$ m/s slugs appear. The roll waves coalesce to form a slug which moves faster than the roll waves (or the base layer suddenly increases to the height required for slugs to grow). The slug overtakes other roll waves and further growth occurs. Fig. 4d shows holdup measurements at a U_{SL} which is slightly above that required for the initiation of slugs. A mixture of roll waves and slugs is observed. However, as already pointed out by Lin and Hanratty (1987a), it is difficult to distinguish between pseudo-slugs and slugs from film height tracings. It could be speculated that a young slug is seen at time $\cong$7 s. This will grow by overtaking the roll wave in front of it.

The compression of the time scale in Fig. 4 distorts the tracings. The heights of the waves in Fig. 4d are about 0.01 m. The wave velocity is about 2 m/s so the distance between the waves is about 2 m. If a slug has a velocity of about 6 m/s, a slug with a length 0.3 m would appear over a time interval of about 0.0 5 s and would be captured by about 20 points. However, a very short newly formed slug with a length of one pipe diameter would be captured by only two points.

4.2. Time mean measurements of the holdup

Measurements of time-mean h/D are presented in Fig. 5. The location of the marking for the initiation of pseudo-slugs was taken from Lin and Hanratty (1987b). This definition is subjective; it is included only to tie the results to previous observations. The measurements of h/D below the transition to slug flow represent the time-averaged height of a stratified wavy flow.

The striking feature of Fig. 5 is the relative insensitivity of holdup to change in U_{SL} in the pseudo-slug regime. For example, at $U_{SG} = 8$ m/s, h/D varies from 0.17 to 0.18 as U_{SL} changes

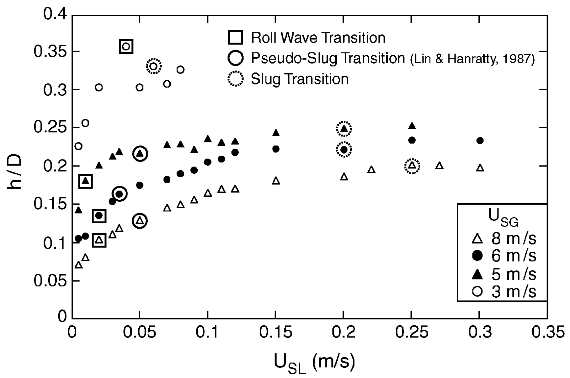

Fig. 5. Holdup at different superficial gas velocities for a range of liquid velocities.

from 0.15 to 0.25 m/s. Measurements of the frequencies of roll waves are given in Fig. 6. These show an increase with increasing U_{SL} in the region where pseudo-slugs exist. The insensitivity of holdup to increases in U_{SL}, therefore, suggests that the volume contained in individual roll waves decreases as the frequency increases. Since the volume flow carried by the roll waves increases with increasing U_{SL}, an insensitivity of holdup would indicate that the velocity of the roll waves are increasing with increasing U_{SL}. Support for this interpretation is obtained from measurements of wave velocities given in Fig. 7.

These could be measured by examining directly the tracings obtained with probes located at 7.92 and 10.36 m from the entrance. In this way the times at which a given roll wave appeared at the two locations were determined and the velocity of the roll wave was calculated as the quotient of the spacing between the probes and the difference in the arrival times. Measurements of the cross-correlation coefficient of the signals from these two probes can also be used. The wave velocity is defined as the ratio of the distance between the probes and the smallest time at which the correlation coefficient reaches a maximum, which is not a large number. Both methods produced approximately the same result.

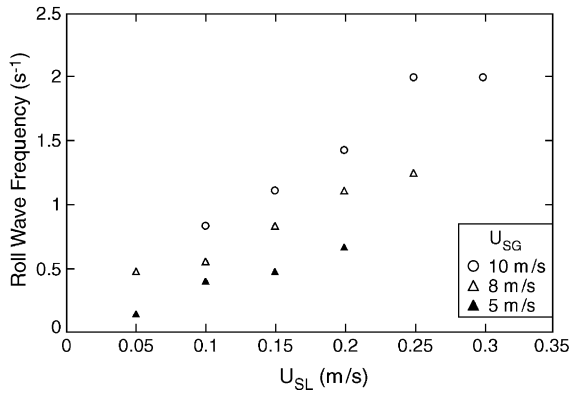

Fig. 6. The effect of liquid superficial velocity on roll wave frequency for different superficial gas velocities.

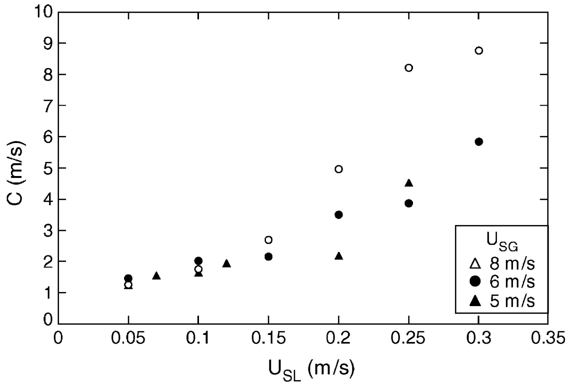

Fig. 7. The effect of U_{SL} on wave velocity for different gas velocities.

4.3. Pressure drops and calculated stresses

Measurements of the mean pressure gradient are presented in Fig. 8. A large increase with increasing U_{SL} is noted in the pseudo-slug region. This arises, mainly, because the increase in U_{SL} is accompanied by an increase in the mean liquid velocity. This, in turn, causes an increase in the wall resistance on the part of the wall that is in contact with the stratified liquid. Another cause could be an increase in the resistance due to the presence of a liquid film on the part of the wall in contact with the gas. These ideas are pursued further by calculating the wall stress, τ_{WL}, and the interfacial stress, τ_i, by using the simplified model of a stratified flow shown in Fig. 1. These calculations are approximate because of shortcomings of the simplified model. The gas–liquid interface is not flat and air could be present in the liquid. Nevertheless, they are used because they provide some help in interpreting the results and because the simplified model is what has been used to calculate U_{SL} when the critical holdup is known.

A force balance relates the pressure drop to the resisting stresses at portions of the wall in contact with the gas, τ_{WG}, and with the liquid, τ_{WL}. The former is calculated by using the Blasius

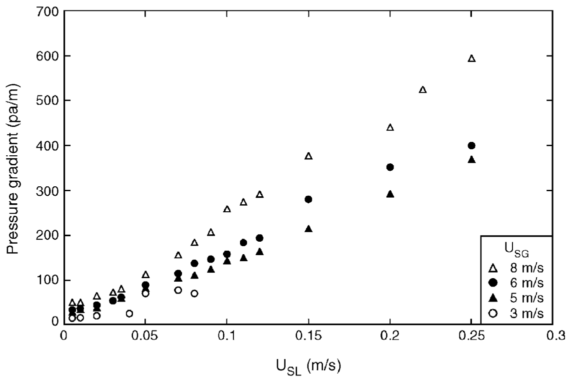

Fig. 8. The effect of superficial liquid velocity on the pressure gradient for a range of superficial gas velocities.

equation. Therefore, measurements of the pressure gradient, Fig. 8, and of h/D, Fig. 5, were used to calculate the τ_{WL} shown in Fig. 9a and b. As expected, the wall resistance increases strongly with increasing U_{SL}. Values of τ_{WL} calculated with the Blasius equation are represented by the curves drawn in Fig. 9a and b. When roll waves are present, τ_{WL} is larger than what is calculated by the Blasuis equation. Results at large U_{SL} can be represented by assuming $f_{WL}/f_{BL} \cong 1.4$ (see Eq. (12)). If an increase in τ_{WG} due to the presence of a wall film were taken into account, the values of τ_{WL} calculated from the measured pressure gradient and h/D would be smaller than given in Fig. 9.

Interfacial stresses, τ_i, were also calculated by using the simple model of a stratified flow (Fig. 1) and by calculating τ_{WG} with the Blasius equation. The values of f_i/f_{BG} in Fig. 10 were obtained from the calculated τ_i and Eqs. (4) and (6). A very large increase in f_i/f_{WB} with increasing U_{SL} is calculated. Values as high as 30 are noted for $U_{SG} = 6$ and 8 m/s close to the transition from a pseudo-slug region to a slug-flow region. These increases can be interpreted as resulting from an increased roughness of the interface due to the presence of waves.

Smaller values of f_i/f_{BG} would be obtained if the calculated τ_{WG} were increased due to the presence of a wall film. However, this would not greatly alter the picture obtained from Fig. 10.

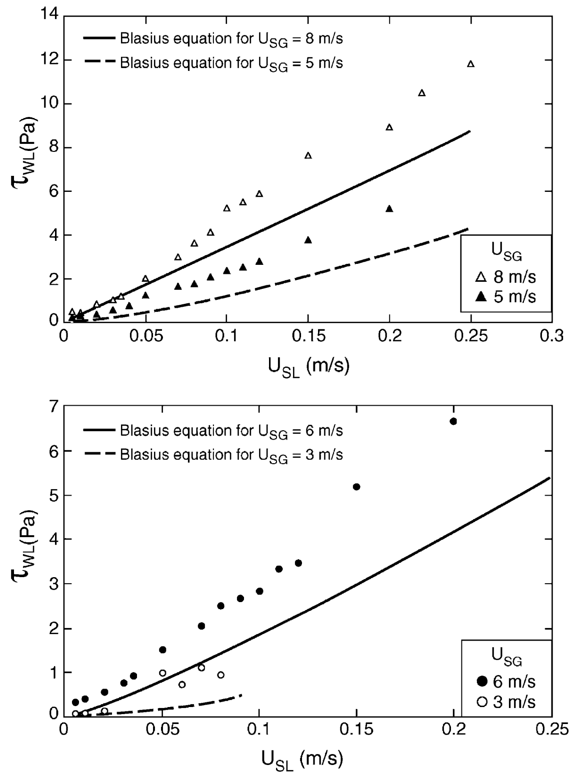

Fig. 9. (a) The effect of U_{SL} on the wall shear stress in the liquid for $U_{SG} = 5$ and 8 m/s. (b) The effect of U_{SL} on the wall shear stress in the liquid for $U_{SG} = 3$ and 6 m/s.

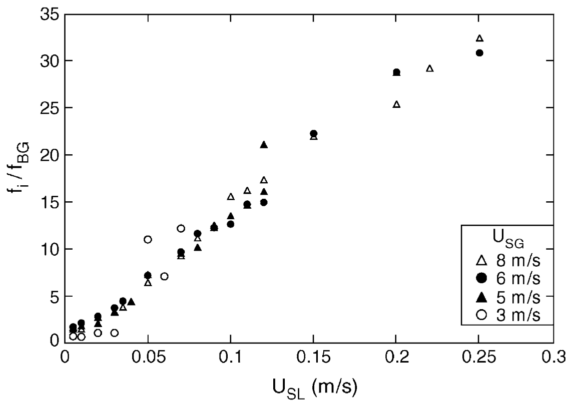

Fig. 10. The interfacial friction factor for a range of superficial liquid velocities at different superficial gas velocities.

5. Comparison with theory

The appearance of roll waves and of slugs are discussed in the preceding section. The critical conditions for the observed transitions are plotted in Figs. 11 and 12. Roll waves appear on a stratified flow with small wavelength waves. The f_i/f_{BG} characterizing the stratified flows at the transition is of the order of 2. The critical h/D and U_{SL} for the appearance of roll waves decrease monotonically with increasing U_{SG}.

The open circles and darkened triangles indicate, respectively, the transition to slugs observed in this study and by Andritsos and Hanratty (1987). At low U_{SG}, where slugs are easily identified, the agreement between the two sets of measurements is good. At large U_{SG} the agreement is as good as can be expected, considering that a certain amount of subjectivity enters into the definition of the transition. At $U_{SG} \leqslant 2$ m/s, the critical U_{SL} for slugging is close to the condition required for the appearance of roll waves. At large U_{SG}, a larger U_{SL} than the critical is required for the transition to slug flow. As already noted in Section 4, Fig. 11 shows that the differences

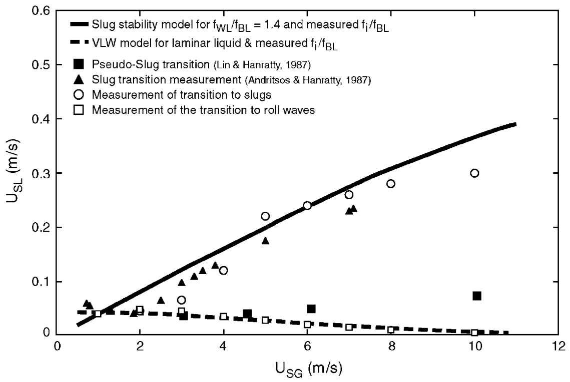

Fig. 11. Critical U_{SL} for air–water flow in a horizontal 2.54 cm pipe.

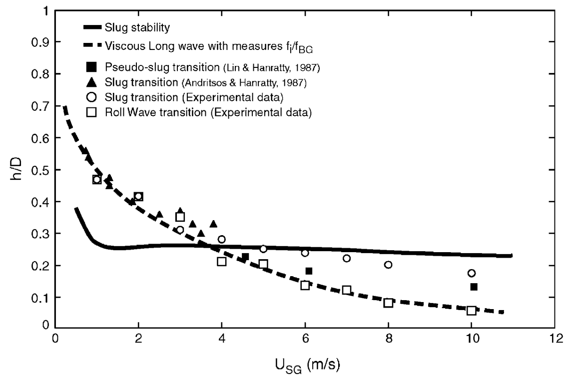

Fig. 12. Critical h/D for air–water flow in a horizontal 2.54 cm pipe.

between the critical U_{SL} for the appearance of slugs and for the appearance of roll waves increases with increasing U_{SG}.

The prediction of instability by VLW theory is given by the gray curves in Figs. 11 and 12. Reynolds numbers for the stratified flow are defined as

$$Re_L = \frac{D_{HL}\rho_L u_L}{\mu_L} \tag{20}$$

where the hydraulic diameter D_{HL} is given as $4A_L/S_L$, u is the average liquid velocity, A_L is the time-averaged area of the liquid and S_L is the length of the pipe circumference which, on average, is in contact with liquid. Calculated Re_L are given in Fig. 13. These support the use of a laminar relation for τ_{WL}, along with measured f_i/f_{BG}, to calculate the critical condition defined by VLW theory. Figs. 11 and 12 show that the VLW theory predicts, quite well, the condition required for the initiation of roll waves (and for the initiation of slugging at low gas velocities).

Predictions of the critical h/D required for the stability of a slug are plotted as the dark lines in Figs. 11 and 12. Eq. (10) was used to calculate τ_{WL} and a value 1.4 was used for f_{WL}/f_{BL}. The

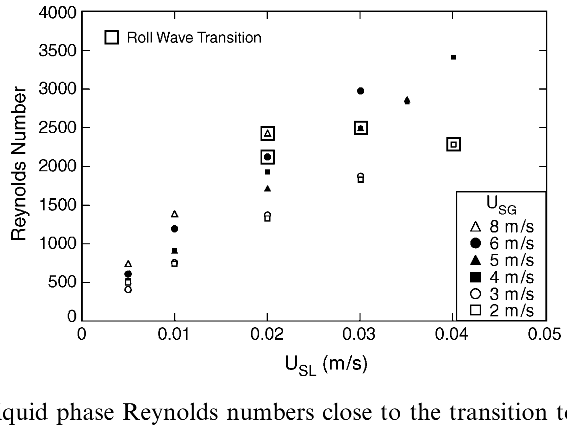

Fig. 13. Liquid phase Reynolds numbers close to the transition to roll waves.

f_i/f_{BG} were taken from the experimental measurements shown in Fig. 10. The appearance of roll waves at higher gas velocities does not lead to the generation of slugs since the height of the stratified flow is not large enough to sustain stable slugs. At U_{SG} larger than 4 m/s, the critical h/D for the transition to slug flow agrees roughly with the theoretical prediction for the stability of slug (see Fig. 12).

As seen in Fig. 11, values of the critical U_{SL} that are calculated with Eqs. (12) and (13) agree, roughly, with the critical U_{SL} observed in laboratory studies.

6. Discussion

A consideration of the stability of a stratified flow with VLW theory and the stability of a slug have provided an explanation for the observed critical liquid height at the transition to slugging for air and water flowing in a horizontal pipe. However, paradoxically, the prediction of the critical superficial liquid velocity has not been so successful (Hurlburt and Hanratty, 2002). This discrepancy provided the motivation for the present study. However, our choice of a 2.54 cm pipe for carrying out the experiments introduced additional complications because there is a large region in which the transition is from the pseudo-slug pattern, defined by Lin and Hanratty (1986, 1987a,b), rather than from a stratified pattern. As a consequence, the explanation of the peculiarities of the transition from pseudo-slugs became a central theme.

One of the contributions of this paper is the demonstration that VLW theory can be used to predict the initiation of roll waves in a pipe flow. This required the assumption of a laminar flow in the stratified layer. The critical height is found to decrease with increasing gas velocity. At low U_{SG} the height is large enough to sustain stable slugs. The transition to slug flow, therefore, occurs at h/D close to that required for the initiation of roll waves because the roll waves have the possibility of growing directly into slugs.

At large U_{SG} the height of the liquid at the transition to roll waves is below the critical height required for the existence of stable slugs. Consequently, there is a large range of liquid flows for which the stratified layer contains roll waves. As the superficial liquid velocity increases the frequency of the roll waves increases (see Fig. 6). This is accompanied by increases in the liquid holdup, the wave velocity and the pressure gradient. A surprising result is that the liquid holdup eventually becomes relatively insensitive to changes in U_{SL}, even though the pressure gradient and wave velocity are increasing. This region of incipient slugging terminates with the appearance of stable slugs.

Thus, it is not sufficient to define the transition to slug flow as occurring when the average holdup of the stratified flow is equal to that predicted for the stability of slugs. A possible reason for this is that the height of the liquid layer between the roll waves is equal to the critical h/D for the initiation of roll waves. This is below that required for a slug to be stable. Therefore, it is not possible for the roll waves to grow directly into slugs. Lin and Hanratty (1987a,b) have observed that the initiation of slugging at high U_{SG} occurs through the coalescence of roll waves. As U_{SL} increases a condition is reached that promotes coalescence. The prediction of the initiation of coalescence, therefore, is needed to predict the critical U_{SL} for initiating slugging. This could depend on the velocity and the frequency of the roll waves.

The marked increase in pressure gradient with increasing U_{SL} (Fig. 7) can be explained by the increase in τ_{WL} associated with the increase of the liquid velocity in the stratified layer. If one uses the simplified model of a slug, shown in Fig. 1, estimates of τ_{WL} and τ_i can be made from measurements of the pressure gradient and the average height of the stratified layer. This indicates that the ratio of interfacial friction factor to the value predicted by the Blasius equation increases with increasing U_{SL} in the region where pseudo-slugs exist. It can assume a value as high as 30 close to the transition to slug flow.

Finally, it is of interest to return to the original motive of this study by examining previous predictions by Hurlburt and Hanratty (2002), of critical U_{SL} for air and water flowing in a horizontal 2.54 cm pipe. As already pointed out, the critical h/D observed in this study agree with the predictions of HH in that they are predicted reasonably well at high gas velocities by considering the stability of slugs and, at low gas velocities, by considering the stability of a stratified flow (see Fig. 12). However, at low U_{SG}, Hurlburt and Hanratty predicted higher U_{SL} than is observed. In their analysis, HH used the Blasius equation to calculate τ_{WL}. Our study shows that better agreement is obtained if the stratified flow is assumed to be laminar. (See the curve in Fig. 11 that is calculated with the VLW model for a laminar liquid.) Another possible explanation, at small U_{SG}, is that an increase in U_{SL} is accompanied by an increase in the hydraulic gradient. This idea could also be pursued.

The calculations by HH, at large U_{SG}, of critical U_{SL} (corresponding to the critical h/D predicted by considering slug stability) are lower than observed. This can be explained because their choices of f_i/f_{BG} are much smaller than observed for incipient slugging. Of course, this result is not surprising. It is expected if one knows the critical h/D and the values of f_i and f_{WL} at transition. The agreement, therefore, does not bypass the need for another physical criterion than slug stability to predict the critical U_{SL} for transition to slug flow from a stratified flow that has pseudo-slugs. As mentioned above, this probably involves a consideration of the initiation of the coalescence of roll waves.

One aspect of the results which is not understood is the observation that the holdup in the region of incipient slugging is close to the critical value needed for the initiation of slugging.

Acknowledgements

This work was supported by the basic Engineering Science Program of the Department of Energy under grant DOE.DEFG02-86ER13556.

References

Andritsos, N., Hanratty, T.J., 1987. Influence of interfacial waves in stratified gas–liquid flows. AIChE J. 33, 444–454.

Andreussi, P., Bendiksen, K., 1989. Investigation of void fractions in liquid slugs for horizontal and inclined gas–liquid pipe flow. Int. J. Multiphase Flow 15, 937–946.

Bendiksen, K.H., 1984. An experimental investigation of the motion of long bubbles in inclined tubes. Int. J. Multiphase Flow 10, 467–483.

Fan, Z., Lusseyran, F., Hanratty, T.J., 1993. Initiation of slugs in horizontal gas–liquid flows. AIChE J. 39, 1741–1753.

Govier, G.W., Aziz, K., 1972. The Flow of complex mixtures in pipes. Van Nostrand Reinhold, New York, p.563.

Hanratty, T.J., Hershman, A., 1961. Initiation of roll waves. AIChE J. 1, 488–497.

Hurlburt, E.T., Hanratty, T.J., 2002. Prediction of the transition from stratified to slug and plug flow in long pipes. Int. J. Multiphase Flow 28, 707–729.

Lin, P.Y., Hanratty, T.J., 1986. Prediction of the initiation of slugs with linear stability theory. Int. J. Multiphase Flow 12, 79–98.

Lin, P.Y., Hanratty, T.J., 1987a. Detection of slug flow from pressure measurements. Int. J. of Multiphase Flow 13, 13–21.

Lin, P.Y., Hanratty, T.J., 1987b. Effect of pipe diameter on flow pattern for air–water flow in horizontal pipes. Int. J. of Multiphase Flow 13, 549–563.

Ruder, Z., Hanratty, P.H., Hanratty, T.J., 1989. Necessary condition for the existence of a stable slug. Int. J. Multiphase Flow 15, 209–226.

Russell, T.W.F., Etchells, A.W., Jensen, R.H., Arruda, P.J., 1974. Pressure drop and holdup in stratified gas–liquid flow. AIChE J. 20, 664–669.

Williams, L.R.,1990. Effect of pipe diameter on horizontal annular two phase flow. Ph.D. thesis, University of Illinois, Urbana.

Woods, B.D., 1998. Slug formation and frequency of slugging in gas–liquid flows. Ph.D. thesis, University of Illinois, Urbana.

Woods, B.D., Hanratty, T.J., 1996. Relation of slug stability to shedding rate. Int. J. Multiphase Flow 22, 809–828.

Wu, H.L., Pots, B.F.M., Hollenburg, J.F., Merhoff, R., 1987. Flow pattern transitions in two-phase gas/condensate flow at high pressure in an 8-inch horizontal pipe. In: Proceedings of the BHRA Conference, The Hague, The Netherlands, pp. 13–21.